Consensus-Based Distributed Intentional Controlled Islanding of Power Grids

Francesco Lo Iudice, *Member, IEEE*, Ricardo Cardona-Rivera, Antonio Grotta, Marco Coraggio, *Member, IEEE*, and Mario di Bernardo, *Fellow, IEEE*

***Abstract*—The problem of partitioning a power grid into a set of islands can be a solution to restore power dispatchment in sections of a grid affected by an extreme failure. Current solutions to this problem usually involve finding the partition of the grid into islands that minimize the sum of their absolute power imbalances. This combinatorial problem is often solved through heuristic centralized methods. In this article, we propose instead a distributed online algorithm through which nodes can migrate among islands, self-organizing the network into a suitable partition. We prove that under a set of appropriate assumptions, the proposed solution yields a partition, whose absolute power imbalance falls within a given bound of the optimal solution. We validate our analytical results by testing our partitioning strategy on the IEEE 118 and 300 benchmark problems.**

***Index Terms*—Decentralized control, islanding, smart grids.**

I. Introduction

THE penetration of renewable and distributed generation, e.g., [1], [2], and [3], and the possible occurrence of cascading failures [4] have made the problem of devising control strategies to govern the operation of power grids of crucial concern. Examples of problems of interest include those reported in [5], [6], [7], [8], [9], [10], [11], and [12].

When the control architecture fails to guarantee reliable operation of the transmission grid, last resort strategies have been devised so as to ensure power dispatchment across at least some of its sections. Strategies for *intentional controlled islanding* (ICI) address this issue [13], [14], [15], [16], [17] by identifying sections of the grid (or *islands*) that can isolate and operate independently from the rest of the network. Recently, intentional islanding has also been proposed in the framework of distribution networks—see [18] and references therein—as the presence of storage devices and renewable energy generation allow these grids to be partitioned into *networks of microgrids*, e.g., [19], [20], and [21]. Finally, sectioning a grid into islands can be instrumental for parallel power system restoration where, to accelerate recovery after a blackout, the islands are restored in parallel and then reconnected [22].

The problem of partitioning a grid into a set of islands (that do not exchange power among each other) is usually posed as a combinatorial problem—see, e.g., [19], [23], [24], and [25]—and sometimes is recast as a graph optimization problem [15], [16], [17]. Solving this problem exactly can be computationally expensive, so that heuristic strategies are frequently used to seek a suboptimal solution, while meeting the required computational time that allows the network to stabilize after a contingency [13], [26], [27], [28]. The centralized techniques used to solve the islanding problem include spectral clustering over simple [22] or multilayer graphs [29], ant colony optimization algorithms [30], or particle swarm optimization [31]. Recently, different scientists and institutions have encouraged a shift toward more distributed operation of the power infrastructure, to facilitate the inclusion of distributed energy resources. Examples include self-organizing capacity for open, distributed, and clean energy communities [32]; changes in the regulatory structure and the role of network operators [33], [34]; and the distributed control of microgrids [35], [36], [37]. To the best of our knowledge, no distributed ICI techniques have been proposed in the current literature.

In this article, we bridge this gap and propose a distributed approach to solve the ICI problem, where network nodes can migrate from an island to another so as to *self-organize* into a partition minimizing the power imbalance between different islands and avoiding large amounts of load shedding. Specifically, starting from some initial partition of the grid, we endow the nodes with the ability of locally estimating the power imbalance of their island and of those neighboring it, and decide whether to migrate or not to a different island from their own.

Manuscript received 23 January 2023; revised 31 March 2023; accepted 23 April 2023. Date of publication 19 May 2023; date of current version 1 March 2024. This work was supported in part by the Research Project PRIN 2017 "Advanced Network Control of Future Smart Grids" funded by the Italian Ministry of University and Research (2020–2023)–http://vectors.dieti.unina.it. Recommended by Associate Editor J. L. Mathieu. *(Corresponding author: Mario di Bernardo.)*

Francesco Lo Iudice is with the Department of Electrical Engineering and Information Technology, University of Naples Federico II, 80138 Naples, Italy (e-mail: francesco.loiudice2@unina.it).

Ricardo Cardona-Rivera is with the Italian Institute of Technology - Center for Translational Neurophysiology, 44121 Ferrara, Italy (e-mail: cardonariveraricardo@gmail.com).

Antonio Grotta and Marco Coraggio are with Scuola Superiore Meridionale, School for Advanced Studies, 80138 Naples, Italy (e-mail: antonio.grotta@unina.it; marco.coraggio@unina.it).

Mario di Bernardo is with the Department of Electrical Engineering and Information Technology, University of Naples Federico II, 80138 Naples, Italy, and also with Scuola Superiore Meridionale, School for Advanced Studies, 80138 Naples, Italy (e-mail: mario.dibernardo@unina.it).

Digital Object Identifier 10.1109/TCNS.2023.3277805

The estimation strategy is completely distributed and decentralized and relies on nodes running a virtual consensus dynamics parameterized so that the consensus equilibrium the nodes reach can be used to estimate the power imbalance of the island of interest. Under suitable assumptions, we analytically show that our migration strategy generates a sequence of partitions that converge in finite time to a configuration, whose average absolute power imbalance falls within a certain bound of the minimal one. We validate our strategy by partitioning the IEEE 118 and IEEE 300 test systems, comparing the viable partitions we obtain to others suggested in previous papers in the literature.

A concise list of our contributions is as follows.

1) We present a novel decentralized consensus-based estimation rule for the nodes of a grid to accurately estimate the power imbalance of the island to which they belong. It is worth noting that our strategy can be applied to estimate any property of a subgraph that is obtained as the sum of the contributions of the nodes belonging to that subgraph. This makes our approach versatile and applicable to a range of scenarios beyond power imbalance estimation.
2) We provide a migration rule allowing the nodes of a grid to self-organize into a partition, whose average power imbalance falls within a precomputable distance from the minimal one.

The rest of this article is organized as follows. In Section II, we introduce some notation and give our problem statement, in Section III we give our decentralized ICI strategy, whose convergence is then proved in Section IV, while its effectiveness is validated numerically in Section V. We then apply our strategy in a realistic case study presenting the results in Section VI, and discuss the perspectives and limitations of our work in Section VII. Finally, Section VIII concludes this article.

II. Preliminaries and Problem Statement

Notation

Given a set $\mathcal{Q}$, we denote by $|\mathcal{Q}|$ its cardinality; $\mathbf{1}$ is the column vector of ones, with appropriate dimension.

1) Power Grid: We model a power grid as an *undirected connected* graph $\mathcal{G} = (\mathcal{V}, \mathcal{E})$, where $\mathcal{V}$ is the set of $n \in \mathbb{N}_{>0}$ grid nodes (loads or generators) and $\mathcal{E}$ is the set of edges representing transmission lines interconnecting them. Without loss of generality, the $n_{\mathrm{g}} \in \mathbb{N}_{>0}$ generators are labeled as nodes $1, \dots, n_{\mathrm{g}}$, while the $n_{\mathrm{l}} \in \mathbb{N}_{>0}$ loads as nodes $n_{\mathrm{g}}+1, \dots, n$. We let $p_i \in \mathbb{R}$ be the active power generated or consumed at node i; $p_i > 0$ if i is a generator, while $p_i \leq 0$ if i is a load. We let A be the (symmetric) adjacency matrix associated with the graph $\mathcal{G}$; its (i,j)th element a_{ij} being 1 if $\{i,j\} \in \mathcal{E}$ or 0 otherwise.

2) Islands and Neighbors: We define an *island* as a connected subgraph $\mathcal{M}_l = (\mathcal{V}_l, \mathcal{E}_l)$ of $\mathcal{G}$, where $\mathcal{V}_l \subseteq \mathcal{V}$ and $\mathcal{E}_l = (\mathcal{V}_l \times \mathcal{V}_l) \cap \mathcal{E}$. Given a set of nodes $\mathcal{V}_l$, we denote by $\mathcal{N}(\mathcal{V}_l)$ the set of *neighbors* of the nodes in $\mathcal{V}_l$, i.e., $\mathcal{N}(\mathcal{V}_l) := \{i \in \mathcal{V} \setminus \mathcal{V}_l \mid \exists j \in \mathcal{V}_l : \{i,j\} \in \mathcal{E}\}$. We say that island $\mathcal{M}_m$ is a *neighbor* of island $\mathcal{M}_l$ if and only if $\mathcal{N}(\mathcal{V}_m) \cap \mathcal{V}_l \neq \varnothing$. Moreover, we denote by $\mathcal{N}_i$ the set of neighbors of node i.

3) Grid Partitions: We say that the grid is *partitioned* into $n_\mu \in \mathbb{N}_{>0}$ islands, described by the subgraphs $\mathcal{M}_l, \dots, \mathcal{M}_{n_\mu}$, with corresponding node sets $\mathcal{V}_1, \dots, \mathcal{V}_{n_\mu}$, if $\Pi = \{\mathcal{V}_1, \dots, \mathcal{V}_{n_\mu}\}$ is a *partition* of $\mathcal{V}$. Additionally, a node, say i, in an island, say $\mathcal{M}_l$, is a *boundary node* if $\mathcal{N}_i \cap (\mathcal{V} \setminus \mathcal{V}_l) \neq \varnothing$. Furthermore, we define the condensed graph $\mathcal{G}^\Pi = (\mathcal{V}^\Pi, \mathcal{E}^\Pi)$ induced by the partition Π, where node l in $\mathcal{V}^\Pi$ is associated with $\mathcal{V}_l$ in Π, and an edge $\{l,m\}$ exists in $\mathcal{E}^\Pi$ if and only if $\mathcal{V}_l \cap \mathcal{N}(\mathcal{V}_m) \neq \varnothing$.

4) Power Imbalance: The *power imbalance* of an island $\mathcal{M}_l$ is defined as

$$P_l := \sum_{i \in \mathcal{V}_l} p_i \tag{1}$$

while the overall *grid's power imbalance* is given by

$$P_{\mathrm{tot}} := \sum_{i=1}^{n} p_i = \sum_{l=1}^{n_\mu} P_l. \tag{2}$$

The power imbalance in (1) is associated with the deviation of the synchronous frequency of the island from its nominal value which, in turn, is related to its stability [9], [38]. Indeed, if the generated power exceeds the loads' demand, the frequency increases, while it decreases otherwise. Excessively large variations in the operating frequency with respect to the nominal one can cause faults.

5) Control Problem: The problem we study is to find a partition of the power grid $\mathcal{G}$ into $n_\mu \geq 2$ islands (that do not exchange power among each other) so as to minimize the *average absolute power imbalance*, defined as

$$J := \frac{1}{n_\mu} \sum_{l=1}^{n_\mu} |P_l|. \tag{3}$$

Note that as $\sum_{l=1}^{n_\mu} |P_l| \geq |\sum_{l=1}^{n_\mu} P_l| = |P_{\mathrm{tot}}|$, then

$$J \geq J^* := \left| \frac{P_{\mathrm{tot}}}{n_\mu} \right|. \tag{4}$$

The cost function in (3) has been used in previous work in the literature on grid partitioning, e.g., [13], [19], and [26], as an indicator of the ability of a power system to satisfy the loads' demand, which is also known as *adequacy* [39].

III. Consensus-Based Partitioning Strategy

We propose a strategy that given an initial partition $\Pi(0)$ of the power grid into n_μ islands, uses a consensus algorithm to let the nodes self-organize into a new partition that minimizes J, as defined in (3). In particular, at each step k of the algorithm, one node can migrate between islands. We denote by $\Pi(k)$ the partition after k migrations have occurred: $\mathcal{M}_l(k) = (\mathcal{V}_l(k), \mathcal{E}_l(k))$, $l \in \{1, \dots, n_\mu\}$ being the corresponding islands; $P_l(k)$, $l \in \{1, \dots, n_\mu\}$ their power imbalances; and $J(k)$ the corresponding value of the cost function.

Our strategy is based on the following two fundamental ingredients:

1) a *distributed dynamic estimator* based on average consensus dynamics that nodes can use to estimate the power imbalance in their island and in those of their neighbors.

2) a *migration condition* according to which a boundary node can decide whether to migrate from its island to a neighboring one.

Next, we describe the two elements above.

A. Distributed Power Imbalance Estimation

At any step k, each node, say i, can obtain an estimate of the power imbalance, say $P_l(k)$, of the island it belongs to or of an island neighboring it, say $\mathcal{M}_l(k) = (\mathcal{V}_l(k), \mathcal{E}_l(k))$, by running a consensus-based estimation strategy.

Specifically, let us define the auxiliary graph $\widehat{\mathcal{M}}_l(k) := (\widehat{\mathcal{V}}_l(k), \widehat{\mathcal{E}}_l(k))$ with

$$\widehat{\mathcal{V}}_l(k) := \begin{cases} \mathcal{V}_l(k) \setminus i, & \text{if } i \in \mathcal{V}_l(k) \\ \mathcal{V}_l(k) \cup i, & \text{if } i \notin \mathcal{V}_l(k) \end{cases} \tag{5}$$

and $\widehat{\mathcal{E}}_l(k) := (\widehat{\mathcal{V}}_l(k) \times \widehat{\mathcal{V}}_l(k)) \cap \mathcal{E}$. To estimate $P_l(k)$, node i must trigger the distributed solution of the two *virtual* continuous-time consensus dynamics given by

$$\dot{x}_h(t) = p_h + \sum_{\{j,h\} \in \mathcal{E}_l(k)} (x_j(t) - x_h(t)), \quad \forall h \in \mathcal{V}_l(k) \tag{6a}$$

$$\dot{\widehat{x}}_h(t) = p_h + \sum_{\{j,h\} \in \widehat{\mathcal{E}}_l(k)} (\widehat{x}_j(t) - \widehat{x}_h(t)), \quad \forall h \in \widehat{\mathcal{V}}_l(k) \tag{6b}$$

starting from null initial conditions. Here, $x_h(t)$ and $\widehat{x}_h(t)$ are the virtual states associated with each node $h \in \mathcal{V}_l(k)$ and $h \in \widehat{\mathcal{V}}_l(k)$, respectively.

Remark 1: To run the consensus dynamics (6) in a distributed manner, we assume the virtual states x_h and $\widehat{x}_h$ are broadcast to all neighboring nodes $\mathcal{N}_h \cap \mathcal{V}_l(k)$.

Now, dynamics (6a) can be recast in matrix form as

$$\dot{\boldsymbol{x}}(t) = \mathbf{p} - L\boldsymbol{x}(t) \tag{7}$$

where $\boldsymbol{x}$ is the stack vector of the virtual states x_h, $\mathbf{p}$ is the stack vector of the power values p_h, and L is the (symmetric) Laplacian matrix associated with $\mathcal{M}_l(k)$. Let us recall that $\mathbf{1}^\mathsf{T}$ is an eigenvector of the symmetric Laplacian L, with 0 as an associated eigenvalue. To obtain the asymptotic behavior of (7), we premultiply (7) by $\mathbf{1}^\mathsf{T}$, obtaining, for all time t

$$\mathbf{1}^\mathsf{T}\dot{\boldsymbol{x}}(t) = \mathbf{1}^\mathsf{T}\mathbf{p} = P_l(k). \tag{8}$$

Moreover, differentiating (7), we obtain the dynamical system $\ddot{\boldsymbol{x}}(t) = -L\dot{\boldsymbol{x}}(t)$, whose dynamics, determined by the spectral properties of L, are such that

$$\lim_{t\to\infty} \dot{\boldsymbol{x}}(t) \in \operatorname{span}(\mathbf{1}). \tag{9}$$

Altogether, (8) and (9) imply that $\lim_{t\to\infty} \dot{\boldsymbol{x}}(t) = \mathbf{1}\omega_l$, where

$$\omega_l := \frac{P_l(k)}{|\mathcal{V}_l(k)|}. \tag{10}$$

Similarly, from (6b), we obtain that $\lim_{t\to\infty} \dot{\widehat{\boldsymbol{x}}}(t) = \mathbf{1}\widehat{\omega}_l$, with

$$\widehat{\omega}_l := \frac{1}{|\widehat{\mathcal{V}}_l(k)|} \sum_{j \in \widehat{\mathcal{V}}_l(k)} p_j. \tag{11}$$

Exploiting (5), (11) can be recast as

$$\widehat{\omega}_l = \begin{cases} \frac{1}{|\mathcal{V}_l(k)|-1} (P_l(k) - p_i), & \text{if } i \in \mathcal{V}_l(k) \\ \frac{1}{|\mathcal{V}_l(k)|+1} (P_l(k) + p_i), & \text{if } i \notin \mathcal{V}_l(k). \end{cases} \tag{12}$$

Then, (10) and (12) can be solved together for the unknowns $P_l(k)$ and $|\mathcal{V}_l(k)|$, obtaining

$$P_l(k) = a_l \omega_l \frac{p_i - \widehat{\omega}_l}{\widehat{\omega}_l - \omega_l} \tag{13a}$$

$$|\mathcal{V}_l(k)| = a_l \frac{p_i - \widehat{\omega}_l}{\widehat{\omega}_l - \omega_l} \tag{13b}$$

with $a_l = -1$ if $i \in \mathcal{V}_l(k)$ and $a_l = 1$ if if $i \notin \mathcal{V}_l(k)$.

From (13a), to estimate $P_l(k)$, node i needs to compute ω_l and $\widehat{\omega}_l$. To do so in a distributed manner, node i starts the distributed computation of the consensus dynamics (6a) and (6b) by broadcasting its virtual states x_i and $\widehat{x}_i$ to the nodes in $\mathcal{N}_i \cap \mathcal{V}_l(k)$. In turn, each of these starts sharing its virtual state with its neighbors (within $\mathcal{V}_l(k)$), until all nodes in $\mathcal{V}_l(k)$ join the distributed simulation. Note that the aforementioned procedure can be conducted through one-hop communication if each node h has knowledge of the index $l \in \{1, \ldots, n_\mu\}$ of the island it belongs to, and of its consumed or generated power p_h. Obviously, in a practical implementation, the grid nodes should be equipped with sufficient computational and communication capabilities to run the virtual consensus dynamics on a timescale that is compatible with the grid requirements.

In what follows, we will show how the network nodes can exploit this estimation process to self-organize into a partition of the power network, whose power imbalance (3) is rendered minimal.

B. Migration Condition

A boundary node (see Section II), say i, in island $\mathcal{M}_m(k)$, can decide whether to migrate to a neighboring island $\mathcal{M}_l(k)$ (see Fig. 1) by assessing the power imbalances $P_l(k)$ and $P_m(k)$ (computed through our estimation strategy in Section III-A).

Specifically, at step k, node i will migrate from $\mathcal{M}_m(k)$ to $\mathcal{M}_l(k)$ if and only if

$$\begin{cases} \min(P_l(k), P_m(k)) < \min(P_l(k+1), P_m(k+1)) & \text{(14a)} \\ \mathcal{M}_m(k+1) \text{ is connected} & \text{(14b)} \end{cases}$$

with

$$P_l(k+1) = P_l(k) + p_i \tag{15a}$$

$$P_m(k+1) = P_m(k) - p_i \tag{15b}$$

$$\mathcal{V}_l(k+1) = \mathcal{V}_l(k) \cup i \tag{15c}$$

$$\mathcal{V}_m(k+1) = \mathcal{V}_m(k) \setminus \{i\}. \tag{15d}$$

Remark 2: Condition (14b) concerning connectivity can be ensured using the estimation strategy in Section III-A. Indeed, given an island $\mathcal{M}_l(k)$, if there exists a node $i \in \mathcal{V}_l(k)$ such that $\mathcal{M}_l(k) \setminus \{i\}$ is not connected, the virtual derivatives $\dot{\widehat{x}}_h$ of its neighbors in $\widehat{\mathcal{M}}_l$ [see (6b)] will in general converge to different values, thus providing a warning signal.

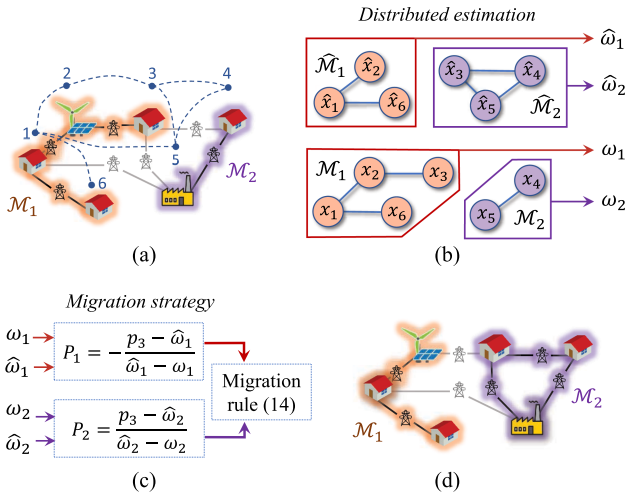

Fig. 1. (a) Initial partition of the power network, with dashed lines representing the communication links among nodes; the topology being equal to that of the power network itself. (b) Boundary node 3 triggers the distributed simulation of the virtual consensus dynamics in (6) for both islands $\mathcal{M}_1$ and $\mathcal{M}_2$. (c) Migration rule (14) is used to decide whether to migrate from island $\mathcal{M}_1$ to $\mathcal{M}_2$ and (d) a new partition is eventually generated.

C. Migration Algorithm

According to our decentralized partitioning strategy, starting from some initial partition at step $k = 0$, each boundary node must trigger the distributed estimation of the power imbalance of the island it belongs to and of its neighboring islands by running the virtual consensus dynamics (6). Then, depending on these power imbalances, exploiting the migration condition (14), the boundary nodes will decide whether to migrate or not to neighboring islands.

For the sake of clarity, we illustrate the process by referring to the exemplary situation depicted in Fig. 1, where a grid with $n = 6$ nodes is initially partitioned in $n_\mu = 2$ islands, $\mathcal{M}_1(0)$ and $\mathcal{M}_2(0)$ [Fig. 1(a)]. Then, each boundary node, as for instance node $3 \in \mathcal{V}_1(0)$, must decide whether to migrate to the other island ($\mathcal{M}_2$) or not. To this aim, node 3 triggers the distributed estimation of the power imbalances $P_1(0)$ and $P_2(0)$ in both the islands $\mathcal{M}_1(0)$ and $\mathcal{M}_2(0)$ [see Fig. 1(b)], by running two virtual consensus processes of the form (6) involving all nodes belonging to each of the islands. Once a steady state in the distributed simulation of (6) has been reached, node 3 uses the pairs $(\omega_1, \hat{\omega}_1)$ and $(\omega_2, \hat{\omega}_2)$ to estimate $P_1(0)$ and $P_2(0)$, which it then uses to evaluate the migration condition (14) [Fig. 1(c)] to assess whether to migrate from $\mathcal{M}_1$ to $\mathcal{M}_2$. Once this decision is taken, a new partition is generated [Fig. 1(d)].

In general, our strategy prescribes that the grid nodes get involved in all the (possibly multiple) distributed consensus processes invoked according to (6) by the boundary nodes of their island or of neighboring ones so as to allow the estimation of the power imbalances of interest. Hence, at any time, each node will have a number of virtual states corresponding to the number of estimation processes it is asked to contribute to. These steps are summarized in Algorithm 1. Additionally, as soon as a node becomes a boundary node (see Section II), it must trigger additional virtual dynamics to decide whether to migrate or not from its island to a neighboring one. This additional procedure is summarized in Algorithm 2.

IV. Proof of Convergence

The following lemma and theorem state that the migration process governed by rule (14) generates a finite sequence $\{\Pi(k)\}_{k\in\{0,\dots,K\}}$ of $K \in \mathbb{N}$ migration steps, and give a bound on the difference between the cost $J(K)$ of the final partition and the optimal cost J^* computed in (4). To give their proof, we must first define the stack vector $\mathbf{P}(k) := [P_1(k) \ \cdots \ P_{n_\mu}(k)]^\mathsf{T}$ and $\mathbf{P}^* := p^*\mathbf{1}$.

Lemma 1: If

$$|P_l(k) - P_m(k)| \le \bar{p} \quad \forall l, m : \mathcal{N}(\mathcal{V}_m(k)) \cap \mathcal{V}_l(k) \neq \varnothing \tag{16}$$

where $\bar{p} := \max_{i\in\mathcal{V}} |p_i|$, then

$$J(k) - J^* \le \frac{2}{n_\mu}\left(\sum_{l=l^*+1}^{n_\mu} p^* + \bar{p}\left(l - \frac{n_\mu+1}{2}\right)\right) - (p^* + |p^*|) \tag{17}$$

with

$$l^* = \left\lceil -\frac{p^*}{\bar{p}} + \frac{n_\mu + 1}{2} \right\rceil \tag{18}$$

and $p^* := P_{\text{tot}}/n_\mu$.

Proof: From (3), we have that

$$J(k) = \frac{1}{n_\mu}\left(\sum_{l:P_l(k)>0} P_l(k) - \sum_{l:P_l(k)\le 0} P_l(k)\right). \tag{19}$$

Moreover, as

$$\sum_{l:P_l(k)>0} P_l(k) + \sum_{l:P_l(k)\le 0} P_l(k) = P_{\text{tot}} = n_\mu p^*$$

we can recast (19) as

$$J(k) = \frac{1}{n_\mu}\left(2\sum_{l:P_l(k)>0} P_l(k) - n_\mu p^*\right).$$

Hence, as $J^* = |p^*|$ [from (4)], we obtain

$$J(k) - J^* = \frac{2}{n_\mu}\sum_{l:P_l(k)>0} P_l(k) - (p^* + |p^*|). \tag{20}$$

Without loss of generality, let us relabel the islands so that $P_1(k) \le P_2(k) \le \cdots \le P_{n_\mu}(k)$. Then, as the graph $\mathcal{G}$ (defined in Section II) and all the islands remain connected for all k, at each step also the graph $\mathcal{G}^{\Pi(k)}$ (defined in Section II) will be connected and thus (16) implies that

$$P_{l+1}(k) \le P_l(k) + \max_{i\in\mathcal{V}} |p_i|, \quad \forall l \in \{1, \dots, n_\mu - 1\}. \tag{21}$$

Note that, from (2), $\sum_{l=1}^{n_\mu} P_l(k) = P_{\text{tot}} = n_\mu p^*$ and, hence, from (21), we obtain

$$P_l(k) \le p^* + \bar{p}\left(l - \frac{n_\mu + 1}{2}\right) \quad \forall l \in \{1, \dots, n_\mu\} \tag{22}$$

with $\bar{p} := \max_{i\in\mathcal{V}} |p_i|$. From (20), $J(k) - J^*$ is maximized (worst case) when (22) is an equality. In such a case, to compute $J(k) - J^*$ by leveraging (20), we must first find

$$l^* : \quad P_l(k) \geq 0, \ \forall l \in \{l^*, \dots, n_\mu\}. \tag{23}$$

Hence, to find l^*, we must find the smallest integer l such that

$$p^* + \bar{p}\left(l - \frac{n_\mu + 1}{2}\right) \geq 0 \tag{24}$$

yielding (18). Then, from (23), (22), and (20), we obtain (17) and the lemma is proved. □

Theorem 1: Assume that at each step k there exist a node i and islands $\mathcal{M}_l(k)$ and $\mathcal{M}_m(k)$ [that is a triplet (l, m, i)] such that

$$\begin{cases} i \in \{\mathcal{V}_m(k) \cap \mathcal{N}(\mathcal{V}_l(k))\} \\ \wedge \\ \mathcal{M}_m(k) \backslash i \text{ is connected} \end{cases} \tag{25a}$$

and

$$\begin{cases} P_l(k) > P_m(k) \ \wedge \ p_i < 0 \\ \vee \\ P_l(k) < P_m(k) \ \wedge \ p_i > 0. \end{cases} \tag{25b}$$

Then, the sequence $\Pi(k)$ obtained under the migration rule (14) is finite and converges in $K < +\infty$ steps to a partition $\Pi(K)$ such that $J(k)$ fulfills (17) at $k = K$.

Proof: Consider a triplet (l, m, i) fulfilling (25), and

$$|P_m(k) - P_l(k)| > |p_i| \tag{26}$$

we start by showing that, when assuming (25), (26) is equivalent to (14), i.e., a migration of node i from island $\mathcal{M}_m$ to $\mathcal{M}_l$ will occur.

Firstly, we show that (14) implies (26). When $P_m(k) < P_l(k)$, we have $p_i < 0$ from (25b), and from (14) we have that

$$P_m(k) < P_l(k+1). \tag{27}$$

Differently, when $P_l(k) < P_m(k)$, we have $p_i > 0$ from (25b), and from (14) we have that

$$P_l(k) < P_m(k+1). \tag{28}$$

From (27) and (28), recalling (15a) and (15b), we have

$$\begin{cases} P_m(k) - P_l(k) < p_i, & \text{if } p_i < 0 \\ P_m(k) - P_l(k) > p_i, & \text{if } p_i > 0. \end{cases} \tag{29}$$

As (29) implies (26), we have proved that (14) implies (26).

Now, let us prove that (26) implies (14). To do so, note that (26) is equivalent to

$$\begin{cases} P_l(k) > P_m(k) + |p_i|, & \text{if } P_l(k) > P_m(k) \\ P_m(k) > P_l(k) + |p_i|, & \text{if } P_l(k) < P_m(k). \end{cases} \tag{30}$$

Moreover, exploiting (25b) and recalling (15a) and (15b), (30) can be recast as

$$\begin{cases} P_m(k) < P_l(k) + p_i = P_l(k+1), & \text{if } P_l(k) > P_m(k) \\ P_l(k) > P_m(k) - p_i = P_m(k+1), & \text{if } P_l(k) < P_m(k). \end{cases} \tag{31}$$

Algorithm 1: Default routine for any node h.

1: Broadcast all virtual states to neighboring nodes
2: Obtain virtual states from neighboring nodes
3: Integrate (6) for all simulations where h is involved

It is straightforward to see that (31) immediately leads to (14). Therefore, we have proved that [when (25) holds] (26)⇔(14). As (14) is equivalent to (26) and (25), then if at some step, say K, no triplet (l, m, i) existed fulfilling (26), the migration process would stop and, as the network $\mathcal{G}$ is connected and so is the graph $\mathcal{G}^{\Pi(K)}$ at that step, we would have

$$|P_l(K) - P_m(K)| \leq \max_{i\in\mathcal{V}} |p_i| \quad \forall l, m : \mathcal{V}_m$$
$$(K) \cap \mathcal{N}(\mathcal{V}_l(K)) \neq \varnothing. \tag{32}$$

As from Lemma 1, (32) implies that the bound (17) holds, to prove our thesis we are left with showing that a stopping time instant K exists. Firstly, note that such a step K exists if (14) fulfills

$$\|\mathbf{P}(k+1) - \mathbf{P}^*\|_2 \leq \alpha \|\mathbf{P}(k) - \mathbf{P}^*\|_2 \ \forall k \in \{0, \dots, K-1\} \tag{33}$$

for some positive scalar $\alpha < 1$ as if (33) were satisfied, then our migration rule would be a contraction mapping. In such case, from the Banach–Caccioppoli theorem [40], there would be no limit cycles in the sequence $\{\mathbf{P}(k)\}$ and thus also in $\{\Pi(k)\}$. Hence, as the number of possible partitions is finite, so would be the sequence $\{\mathbf{P}(k)\}$ and thus, to complete our proof, we need to show that (14) implies (33). As we have enforced that only one migration occurs at each step k, then $\mathbf{P}(k+1)$ only differs from $\mathbf{P}(k)$ for the lth and mth entries. Hence, proving (33) only requires showing that

$$(P_l(k+1) - p^*)^2 + (P_m(k+1) - p^*)^2$$
$$< (P_l(k) - p^*)^2 + (P_m(k) - p^*)^2 \tag{34}$$

for all $k \in \{0, \dots, K-1\}$. After a few algebraic simplifications, (34) can be rewritten as

$$p_i(P_l(k) - P_m(k) + p_i) < 0 \quad k \in \{0, \dots, K-1\} \tag{35}$$

which is trivially fulfilled by any triplet (l, m, i) fulfilling (25) and (26), yielding that (25) and (26) imply (33). In turn, as (25) and (26) imply (14), the existence of K and thus our thesis remains proved. □

Remark 3: A sufficient (but not necessary) condition to fulfill the assumption of Theorem 1 is that neighboring islands have at least a load on the boundary between them.

In the following section, we validate the strategy numerically.

V. Numerical Validation

We demonstrate the effectiveness of our algorithm by deploying it to partition the IEEE 118 and 300 testbed cases [41]. The nodal power values p_i are computed by solving an optimal power flow (OPF) problem on the whole nonpartitioned grid, leveraging MATPOWER 6.0 [42]. As the test cases include nodes with null nodal power $p_i = 0$, we allow for these nodes to

Algorithm 2: Additional steps for a *boundary node* $h \in \mathcal{V}_m$.

Communicate with the nodes in $\mathcal{N}_h \cap \mathcal{V}_m$ to trigger a distributed simulation of (6)
for $l : \mathcal{N}_h \cap \mathcal{V}_l \neq \varnothing$ **do**
  Communicate with the nodes in $\mathcal{N}_h \cap \mathcal{V}_l$ to trigger a distributed simulation of (6)
  Wait for steady state in such simulations
  Estimate P_m and P_l, $\forall l : \mathcal{N}_h \cap \mathcal{V}_l \neq \varnothing$ using (13)
  Decide whether to migrate from $\mathcal{M}_m$ to $\mathcal{M}_l$ via (14)

migrate from their island, say $\mathcal{M}_m(k)$, to a neighboring island, say $\mathcal{M}_l(k)$, as long as: 1) their migration does not render $\mathcal{M}_m(k)$ disconnected and 2) $P_l(k) \neq P_l(k')\forall k' < k : i \in \mathcal{V}_l(k')$.

To apply our partitioning strategy (Algorithms 1 and 2), we need some initial partitions $\Pi(0)$. To test our algorithm under different conditions, we considered different choices for $\Pi(0)$. In some cases, we took as $\Pi(0)$ some selected partitions from [13], [27], and [43]. In other cases, to generate $\Pi(0)$, we first employ the search space reduction procedure (SSRP) [27], which generates a spanning tree connecting groups of coherent generators (these are taken from [27]). Then, the remaining nodes are aggregated to the tree using the breadth-first search (BFS) algorithm [44].

Remark 4: Throughout our numerical analysis, whenever a node, say $i \in \mathcal{V}_m(k)$, can choose to migrate to more than one island, it will select the one maximizing the difference

$$\Delta P_l = \min\{P_l(k)+P_i, P_m(k)-P_i\} - \min\{P_l(k), P_m(k)\}.$$

This choice ensures a maximal improvement of the average absolute power imbalance after the migration.

A. IEEE 118 bus System

We used our algorithm to partition the IEEE 118 test system in $n_\mu = 2$ and $n_\mu = 3$ islands, considering only $n_g = 19$ generators (excluding the reactive compensators). We assume that the migration process is triggered by a three-phase solid ground fault at bus 15 forcing lines 14 and 15 to disconnect. With $n_\mu = 2$, we ran the algorithm first by considering as initial partition $\Pi(0)$, the one generated by SSRP+BFS, and then using as $\Pi(0)$ the final partition reported in [13] to evaluate how it performed when started from different initial partitions. For the case $n_\mu = 3$, we considered as $\Pi(0)$ the partition generated via SSRP+BFS and then the final one obtained in [27]. All relevant information and the results of our distributed partitioning strategy are reported in Table I.

We observe that the proposed algorithm is indeed capable of converging in all cases towards partitions that minimize J, as $J(K) = J^*$. As a representative example, we depict in Fig. 2 the case that $n_\mu = 2$ and $\Pi(0)$ is generated by SSPR+BFS; namely, Fig. 2(a) portrays the power imbalances $P_1(k)$ and $P_2(k)$ at the various steps, while the final partition $\Pi(K)$ is reported in Fig. 2(b). Note that from the OPF results we have $\max_i |p_i| = 542.78$ MW and $J^* = 58.25$ MW and thus the bound given in Theorem 1 is satisfied as $|J(K) - J^*| = 0$ (see Table I).

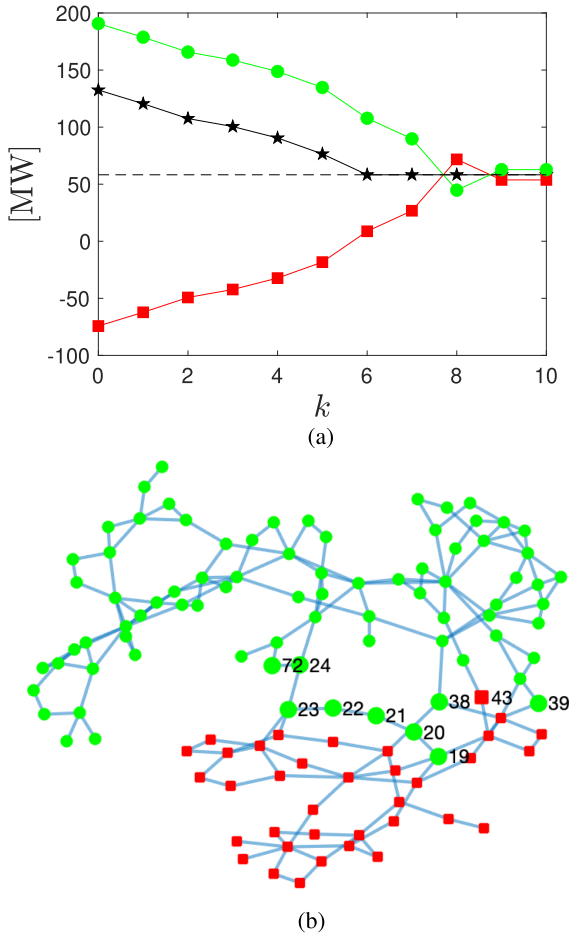

Fig. 2. Partitioning of the IEEE 118 test system into $n_\mu = 2$ islands, through Algorithms 1 and 2. (a) $P_1(k)$ (red squares), $P_2(k)$ (green circles), $J(k)$ (black stars), and J^* (dashed line); all are in MW. (b) Final network partition $\Pi(K)$; red square denote $\mathcal{V}_1(K)$, while green circles denote $\mathcal{V}_2(K)$. Nodes 72, 24, 23, 22, 21, 39, 20, 19, 38 migrated from $\mathcal{M}_1$ to $\mathcal{M}_2$ in the given order, while node 43 migrated from $\mathcal{M}_2$ to $\mathcal{M}_1$ at $k = 9$. Note that the last migration does not change the power imbalances as it involves node 38 whose nodal power is zero.

B. IEEE 300 bus System

We used Algorithms 1 and 2 to partition the IEEE 300 test system in $n_\mu = 3$ and in $n_\mu = 4$ islands, assuming a failure affects lines 194 and 195. With $n_\mu = 3$, as $\Pi(0)$ we considered the partition obtained via SSRP+BFS. We also repeat the partitioning starting from the arbitrary initial partition reported in Table II. When $n_\mu = 4$, as initial partition $\Pi(0)$ we consider one obtained via SSRP+BFS and one from [27]. In both cases, the groups of coherent generators were selected as in Table II of [27]. All relevant information and the results are reported in Table II.

Again, in all cases, our algorithm is capable of finding an optimal partition, as $J(K) = J^*$. Additionally, we note that the initial partitions obtained via SSRP+BFS and that from [27] are already optimal with respect to minimizing J; however, by performing a few more migration steps, our algorithm is able to further decrease the standard deviation between the power imbalances of the three islands (compare $P_l(0)$ and $P_l(K)$ in Table II). This happens routinely, as the migration law (14) aims

TABLE I
RESULTS AFTER APPLYING ALGORITHMS 1 AND 2 TO THE IEEE 118 TEST CASE, CONSIDERING DIFFERENT INITIAL PARTITIONS $\Pi(0)$

Case	n_μ	K	Cut-set at $\Pi(0)$	$\Pi(0)$	Cut-set at $\Pi(K)$	$J(0)$	$J(K)$	J^*	$P_l(0)$	$P_l(K)$	Bound (17)
IEEE 300	3	3	{3-129, 7-110, 40-68, 54-123, 57-66, 66-190, 67-190, 68-73, 185-186}	SSRP+BFS	{3-129, 40-68, 54-123, 57-66, 64-67, 66-190, 68-73, 109-110, 184-185, 185-187}	102.92	102.92	102.92	{6.11, 129.98, 172.65}	{6.11, 145.98, 156.65}	1254.95
IEEE 300	3	12	{40-68, 57-66, 66-190, 67-190, 68-73, 106-113, 112-116, 122-123, 185-186}	Arbitrary	{36-40, 39-40, 61-66, 64-67, 65-66, 68-73, 105-106, 106-107, 106-147, 112-116, 119-121, 121-154, 122-124, 122-128, 127-157, 154-158, 157-158, 168-189, 172-187, 177-188, 184-185}	529.49	102.92	102.92	{−639.87, 775.96, 172.65}	{129.21, 18.89, 160.65}	1254.95
IEEE 300	4	5	{3-129, 7-110, 40-68, 54-123, 61-66, 64-67 65-66, 68-73, 68-173, 174-198, 185-186}	SSRP+BFS	{3-129, 7-110, 40-68, 54-123, 57-180, 57-190, 66-190, 67-190, 68-73, 68-173, 168-187, 172-187, 174-198, 184-185}	77.187	77.187	77.187	{19.76, 6.11, 205.98, 76.9}	{114.76, 6.11, 110.98, 76.9}	1908.2
IEEE 300	4	3	{57-66, 64-67, 66-190, 68-173, 109-110, 109-129, 122-123, 174-191, 174-198, 184-185, 185-187}	[27]	{7-110, 57-66, 66-190, 67-190, 68-173, 109-129 122-123, 168-187, 172-187, 174-191, 174-198, 184-185}	77.187	77.187	77.187	{145.98, 79.76, 6.11 76.9}	{110.98, 114.76, 6.11, 76.9}	1908.2

Power values are reported in MW.

TABLE II
RESULTS AFTER APPLYING ALGORITHMS 1 AND 2 TO THE IEEE 300 TEST CASES, CONSIDERING DIFFERENT INITIAL PARTITIONS $\Pi(0)$

Case	n_μ	K	Cut-set at $\Pi(0)$	$\Pi(0)$	Cut-set at $\Pi(K)$	$J(0)$	$J(K)$	J^*	$P_l(0)$	$P_l(K)$	Bound (17)
IEEE 300	3	3	{3-129, 7-110, 40-68, 54-123, 57-66, 66-190, 67-190, 68-73, 185-186}	SSRP+BFS	{3-129, 40-68, 54-123, 57-66, 64-67, 66-190, 68-73, 109-110, 184-185, 185-187}	102.92	102.92	102.92	{6.11, 129.98, 172.65}	{6.11, 145.98, 156.65}	1254.95
IEEE 300	3	12	{40-68, 57-66, 66-190, 67-190, 68-73, 106-113, 112-116, 122-123, 185-186}	Arbitrary	{36-40, 39-40, 61-66, 64-67, 65-66, 68-73, 105-106, 106-107, 106-147, 112-116, 119-121, 121-154, 122-124, 122-128, 127-157, 154-158, 157-158, 168-189, 172-187, 177-188, 184-185}	529.49	102.92	102.92	{−639.87, 775.96, 172.65}	{129.21, 18.89, 160.65}	1254.95
IEEE 300	4	5	{3-129, 7-110, 40-68, 54-123, 61-66, 64-67 65-66, 68-73, 68-173, 174-198, 185-186}	SSRP+BFS	{3-129, 7-110, 40-68, 54-123, 57-180, 57-190, 66-190, 67-190, 68-73, 68-173, 168-187, 172-187, 174-198, 184-185}	77.187	77.187	77.187	{19.76, 6.11, 205.98, 76.9}	{114.76, 6.11, 110.98, 76.9}	1908.2
IEEE 300	4	3	{57-66, 64-67, 66-190, 68-173, 109-110, 109-129, 122-123, 174-191, 174-198, 184-185, 185-187}	[27]	{7-110, 57-66, 66-190, 67-190, 68-173, 109-129 122-123, 168-187, 172-187, 174-191, 174-198, 184-185}	77.187	77.187	77.187	{145.98, 79.76, 6.11 76.9}	{110.98, 114.76, 6.11, 76.9}	1908.2

Power values are reported in MW.

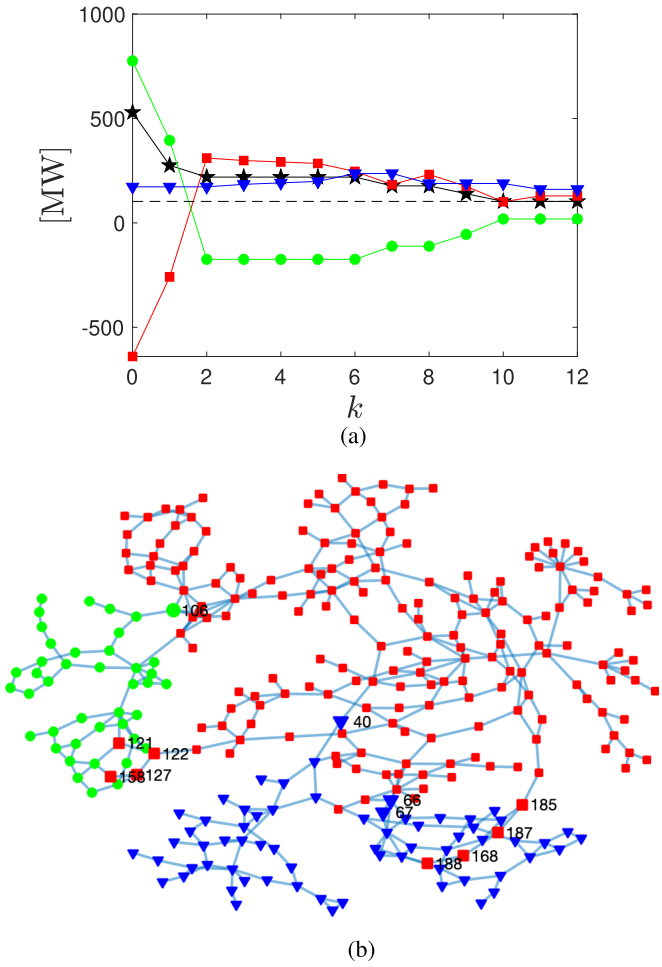

Fig. 3. Partitioning of the IEEE 300 test system into $n_\mu = 3$ islands, through Algorithms 1 and 2. (a) $P_1(k)$ (red squares), $P_2(k)$ (green circles), $P_3(k)$ (blue triangles), $J(k)$ (black stars), and J^* (dashed line). (b) Final network partition $\Pi(K)$; red squares denote $\mathcal{V}_1(K)$, green circles denote $\mathcal{V}_2(K)$, and blue triangles denote $\mathcal{V}_3(K)$. The nodes' migration order is 106, 122, 185, 187, 168, 188, 127, 66, 121, 158, 67, and 40.

at equalizing the power imbalances in all the islands (with the result of minimizing J).

In Fig. 3, we report the representative case where $n_\mu = 3$ and $\Pi(0)$ is the arbitrary partition. The power imbalances $P_1(k)$, $P_2(k)$, and $P_3(k)$ are depicted in Fig. 3(a), while the final partition $\Pi(K)$ is portrayed in Fig. 3(b). Interestingly, across all our numerical experiments, not only does our algorithm ensure fulfillment of the bound given in Theorem 1, but it also always ensures $J(K) = J^*$, and in all cases it succeeds in reducing the standard deviation among the power imbalances of the islands with respect to that of the initial partition (see Table II).

VI. Case Study

As shown in our numerical analysis, our decentralized strategy is not only capable of minimizing (3), but also of diminishing the standard deviation between power imbalances, thus making the islands equally robust to unforeseen power fluctuations. Unsurprisingly, this comes at the price of cutting several lines, as minimization of the power imbalance and of the *power flow disruption* are known to be conflicting goals [13]. While both could benefit from some load shedding, ultimately, a partition with high power imbalance and/or power flow disruption leads to the existence of islands where the the power flow is unfeasible and thus loads will not be served. Our migration strategy does not take explicitly into account the number of lines cut. We present here a case study to show that, nevertheless, it can still lead to nodes self-organizing into a partition where power is not only available but can be dispatched, i.e., the power flow is feasible for all the islands.

To this aim, we consider the problem of refining the partition of the IEEE 118 test case into $n_\mu = 3$ islands proposed in [27], to react to a failure in bus 26.[1] Solving the power flow for the test case in the absence of a fault shows that this generator is responsible for 7.2% of the total active power generated and, consistently, postfault, an island of the partition will be endowed with negative power imbalance. To overcome this problem, we apply our strategy using the partition proposed in [27] as initial partition $\Pi(0)$ for our distributed algorithm. We take the groups of coherent generators as in [27], this time assuming these nodes cannot change island throughout the migration process. Furthermore, following [22], we assume that postfault load can be shed by 15%[2] in noncritical loads belonging to islands affected by the refinement process, and select the set of critical loads as in [22]. Finally, as our aim is that of refining $\Pi(0)$ so as to make sure all islands are such that $P_l(K) \geq 0$, we enforce the additional rule that node i can migrate from $\mathcal{M}_m(k)$ to $\mathcal{M}_l(k)$ only if $\text{sign}(P_l(k)) = -\text{sign}(P_m(k))$ which will cause migrations to cease if all islands have positive power imbalance. To evaluate the quality of the partition $\Pi(K)$ resulting from applying our strategy, we will compare the properties of the power flow solutions of the islands in $\Pi(K)$ to those in $\Pi(0)$ in terms of

1) minimal and maximal voltage magnitude $V_{\min}$ and $V_{\max}$;
2) minimal and maximal voltage angles $\delta_{\min}$ and $\delta_{\max}$;
3) active and reactive power losses λ_P and λ_Q.

We find that in this scenario $K = 17$ migrations are required to make sure all islands have positive power imbalance, resulting in the nodes self-organizing into a partition defined by the cutset {15-19, 17-113, 18-19, 23-25, 27-32, 31-32, 34-37, 35-37,37-39, 37-40, 38-65, 69-77, 75-77, 76-118, 80-81, 114-115}. Let us start describing the outcome of our case-study underlining that $\mathcal{V}_3(K) = \mathcal{V}_3(0)$, i.e., no migrations occurred that changed island $\mathcal{M}_3$. For this reason, we shed no load in this island postfault, resulting in no changes in its power flow. Conversely, all 17 migrations involve nodes in islands $\mathcal{M}_1$ and $\mathcal{M}_2$. Consistently, as shown in Table III, for these two islands we observe changes in all the variables we chose to describe the power flow solution. However, the only variable whose value degrades substantially is the worst minimal voltage magnitude $V_{\min}$ that, for island $\mathcal{M}_2(k)$ takes the value of 0.87, quite far from the desired value of 1 and lower than the initial value of 0.946, but still consistent with other islanding results available in the literature (see for instance Fig. 4 in [45]). Conversely, the largest

[1]For the purpose of this case study, it is irrelevant whether islanding is performed to avoid a blackout or for parallel power grid restoration purposes.

[2]This value is half that considered in [22] when solving the islanding problem for Parallel Power System Restoration.

TABLE III
COMPARISON BETWEEN THE PROPERTIES OF THE POWER FLOW SOLUTION PREFAULT FOR THE ISLANDS DEFINED BY THE INITIAL PARTITION $\Pi(0)$ DEFINED IN [27] AND POSTFAULT AFTER THE INITIAL PARTITION IS REFINED THROUGH OUR DISTRIBUTED STRATEGY

Island	P_l [MW]	$V_{\min}$ [p.u.]	$V_{\max}$ [p.u.]	$\delta_{\min}$ [deg]	$\delta_{\max}$ [deg]	λ_P [MW]	λ_Q [MVar]
$\mathcal{M}_1(0)$	−410	0.936	1.050	−20.66	21.25	6.27	59.22
$\mathcal{M}_2(0)$	474	0.946	1.050	17.47	32.61	6.32	19.03
$\mathcal{M}_3(0)$	216	0.943	1.040	17.13	41.77	3.96	20.18
$\mathcal{M}_1(K)$	14	0.955	1.050	8.51	33.68	4.94	59.22
$\mathcal{M}_2(K)$	58	0.874	1.050	−44.47	30.27	16.74	70.87
$\mathcal{M}_3(K)$	216	0.943	1.040	17.13	41.77	3.96	20.18

voltage angle (in magnitude) is comparable before and after the migration process, and while we observe a general increase in the active and reactive losses, the highest reactive power loss in the final partition is just 20% larger than that prefault.

Overall, this case study shows that our strategy can also be deployed for postfault refinement of a reasonable partition. Next, we discuss the steps required towards a real-world implementation of such a decentralized islanding strategy.

VII. TOWARD A PRACTICAL IMPLEMENTATION

In this section, we discuss some issues that are important to achieve a practical implementation of the strategy.

A. Power Flow Feasibility

In this work, we chose to seek a partition of a grid that minimizes the islands' power imbalance. As is known in the literature [13], this can come at the price of obtaining a large power flow disruption which can cause the power flow to be unfeasible for some of the islands. However, this choice allowed us to prove rigorously that nodes of a power system can self-organize into islands that fulfill some electrical property of interest.

The test case described in Section VI shows that our results can also be exploited in a realistic scenario. Nevertheless, for practical implementation, power flow disruption should also be explicitly taken into account to systematically ensure the available power to be dispatchable. We are currently adapting the tools developed in this work to optimize the tradeoff between power imbalance and the power flow disruption. Our preliminary numerical investigations are encouraging, and suggest that a multiobjective distributed strategy based on the same estimation tools presented in this work can consistently lead to islands where power is both available and can be dispatched.

B. Implementation Issues

A real world implementation of the tools presented in this article relies on the following three assumptions: 1) the availability of computational power at each node; 2) the availability of a communication infrastructure between the nodes having the same topology as the physical grid and 3) the availability of measurements of the generated/consumed power at each node. Which one of these assumptions proves more restrictive depends on the reason for which islanding is needed. In case islanding is needed to avoid a cascading outage, the largest drawback with respect to a centralized approach is that substantial effort must be devoted in designing efficient distributed simulation protocols. Indeed, to avoid a blackout, the migration process must be executed on a timescale compatible with that of the development of postfault instability. In our numerical experiments, we found that the numerical simulations required to perform a migration step lasted around 8 ms to run (on a personal computer equipped with an Intel Core i5 processor with six cores at 3 GHz, and 16 GB of RAM memory) yielding, for the test case in Section VI, and a total time of 0.12 s for the nodes to obtain the final partition. Note that this is in line with the computational time required to solve the islanding problem on the same test case (the IEEE 118 bus system) in [46].

If the strategy is applied for parallel power system restoration, i.e., post black-out, ensuring reliable communication among the nodes might be the most pressing issue.

Finally, in energetic communities, privacy issues may arise and one might want to make sure nodes cannot infer the power generated or absorbed by their peers from the communicated signals. Furthermore, in this latter case, choosing the number of energetic communities n_μ could also be exploited for optimization purposes, whereas in postfault scenarios it is usually fixed and determined by the groups of coherent generators and, for the case of parallel power system restoration, by the availability of blackstart units. Addressing these issues is the subject of ongoing work and will be reported elsewhere.

C. Limitations

Although the framework we have developed offers several advantages, such as effective power management and fault tolerance, it does have a significant limitation. Specifically, it requires an external initial partition to be provided, which could be a potential bottleneck in the decentralization process. While it is realistic to assume the availability of such a partition, fully decentralizing the islanding process would necessitate the development of a distributed strategy enabling generators to self-organize into coherent groups and recursively add loads to form the initial islands. Addressing this limitation is an important direction for future research, as it could lead to greater efficiency and scalability of the overall system.

VIII. CONCLUSION

We introduced a power network islanding algorithm that solves the intentional controlled islanding problem in a distributed manner. Our strategy allows the network nodes to self-organize so as to minimize the average absolute power imbalance among islands. To allow the nodes to make informed decisions, we devised a consensus-based estimator which is instrumental to the migration process, as it allows nodes to estimate the power imbalances of neighboring islands in a distributed manner. We demonstrated analytically that our algorithm converges in finite time to a partition whose average absolute power imbalance

is in a given neighborhood of the optimal one. We tested the strategy on two benchmark power networks, the IEEE 118 and 300 bus systems under different fault conditions showing the effectiveness of the proposed approach.

REFERENCES

[1] F. Dörfler, J. W. Simpson-Porco, and F. Bullo, "Breaking the hierarchy: Distributed control and economic optimality in microgrids," *IEEE Trans. Control Netw. Syst.*, vol. 3, no. 3, pp. 241–253, Sep. 2016.

[2] A. Bidram and A. Davoudi, "Hierarchical structure of microgrids control system," *IEEE Trans. Smart Grid*, vol. 3, no. 4, pp. 1963–1976, Dec. 2012.

[3] P. Frasca, H. Ishii, C. Ravazzi, and R. Tempo, "Distributed randomized algorithms for opinion formation, centrality computation and power systems estimation: A tutorial overview," *Eur. J. Control*, vol. 24, pp. 2–13, 2015.

[4] P. Pourbeik, P. S. Kundur, and C. W. Taylor, "The anatomy of a power grid blackout-root causes and dynamics of recent major blackouts," *IEEE Power Energy Mag.*, vol. 4, no. 5, pp. 22–29, Sep./Oct. 2006.

[5] J. Rocabert, A. Luna, F. Blaabjerg, and P. Rodriguez, "Control of power converters in AC microgrids," *IEEE Trans. Power Electron.*, vol. 27, no. 11, pp. 4734–4749, Nov. 2012.

[6] A. Tayyebi, D. Groß, A. Anta, F. Kupzog, and F. Dörfler, "Frequency stability of synchronous machines and grid-forming power converters," *IEEE Trans. Emerg. Sel. Topics Power Electron.*, vol. 8, no. 2, pp. 1004–1018, Jun. 2020.

[7] C. Arghir, T. Jouini, and F. Dörfler, "Grid-forming control for power converters based on matching of synchronous machines," *Automatica*, vol. 95, pp. 273–282, 2018.

[8] F. Milano, F. Dörfler, G. Hug, D. J. Hill, and G. Verbič, "Foundations and challenges of low-inertia systems," in *Proc. IEEE Power Syst. Comput. Conf.*, 2018, pp. 1–25.

[9] F. Dörfler, S. Bolognani, J. W. Simpson-Porco, and S. Grammatico, "Distributed control and optimization for autonomous power grids," in *Proc. IEEE 18th Eur. Control Conf.*, 2019, pp. 2436–2453.

[10] G. Lalor, A. Mullane, and M. O'Malley, "Frequency control and wind turbine technologies," *IEEE Trans. Power Syst.*, vol. 20, no. 4, pp. 1905–1913, Nov. 2005.

[11] H. Bevrani, A. Ghosh, and G. Ledwich, "Renewable energy sources and frequency regulation: Survey and new perspectives," *IET Renewable Power Gener.*, vol. 4, no. 5, pp. 438–457, 2010.

[12] A. Ulbig, T. S. Borsche, and G. Andersson, "Impact of low rotational inertia on power system stability and operation," *IFAC Proc. Volumes*, vol. 47, no. 3, pp. 7290–7297, 2014.

[13] X. Fan, E. Crisostomi, D. Thomopulos, B. Zhang, and S. Yang, "A controlled islanding algorithm for AC/DC hybrid power systems utilizing dc modulation," *IET Gener., Transmiss. Distrib.*, vol. 14, no. 26, pp. 6440–6449, 2020.

[14] S. Pahwa, M. Youssef, P. Schumm, C. Scoglio, and N. Schulz, "Optimal intentional islanding to enhance the robustness of power grid networks," *Physica A, Stat. Mechanics Appl.*, vol. 392, no. 17, pp. 3741–3754, 2013.

[15] K. Sun, D.-Z. Zheng, and Q. Lu, "Splitting strategies for islanding operation of large-scale power systems using OBDD-based methods," *IEEE Trans. Power Syst.*, vol. 18, no. 2, pp. 912–923, May 2003.

[16] M. Adibi, R. Kafka, S. Maram, and L. M. Mili, "On power system controlled separation," *IEEE Trans. Power Syst.*, vol. 21, no. 4, pp. 1894–1902, Nov. 2006.

[17] P. Fernández-Porras, M. Panteli, and J. Quirós-Tortós, "Intentional controlled islanding: When to island for power system blackout prevention," *IET Gener., Transmiss. Distrib.*, vol. 12, no. 14, pp. 3542–3549, 2018.

[18] A. R. H. Ahangar, G. B. Gharehpetian, and H. R. Baghaee, "A review on intentional controlled islanding in smart power systems and generalized framework for ICI in microgrids," *Int. J. Elect. Power Energy Syst.*, vol. 118, 2020, Art. no. 105709.

[19] H. Haddadian and R. Noroozian, "Multi-microgrids approach for design and operation of future distribution networks based on novel technical indices," *Appl. Energy*, vol. 185, pp. 650–663, 2017.

[20] Z. Wang, B. Chen, J. Wang, M. M. Begovic, and C. Chen, "Coordinated energy management of networked microgrids in distribution systems," *IEEE Trans. Smart Grid*, vol. 6, no. 1, pp. 45–53, Jan. 2015.

[21] S. A. Arefifar and Y. A.-R. I. Mohamed, "DG mix, reactive sources and energy storage units for optimizing microgrid reliability and supply security," *IEEE Trans. Smart Grid*, vol. 5, no. 4, pp. 1835–1844, Jul. 2014.

[22] J. Quirós-Tortós, P. Wall, L. Ding, and V. Terzija, "Determination of sectionalising strategies for parallel power system restoration: A spectral clustering-based methodology," *Electric Power Syst. Res.*, vol. 116, pp. 381–390, 2014.

[23] S. A. Arefifar, A.-R. M. Yasser, and T. H. El-Fouly, "Optimum microgrid design for enhancing reliability and supply-security," *IEEE Trans. Smart Grid*, vol. 4, no. 3, pp. 1567–1575, Sep. 2013.

[24] S. Hasanvand, M. Nayeripour, E. Waffenschmidt, and H. Fallahzadeh-Abarghouei, "A new approach to transform an existing distribution network into a set of micro-grids for enhancing reliability and sustainability," *Appl. Soft Comput.*, vol. 52, pp. 120–134, 2017.

[25] S. Mohammadi, S. Soleymani, and B. Mozafari, "Scenario-based stochastic operation management of microgrid including wind, photovoltaic, micro-turbine, fuel cell and energy storage devices," *Int. J. Elect. Power Energy Syst.*, vol. 54, pp. 525–535, 2014.

[26] Z. Liu, A. Clark, L. Bushnell, D. S. Kirschen, and R. Poovendran, "Controlled islanding via weak submodularity," *IEEE Trans. Power Syst.*, vol. 34, no. 3, pp. 1858–1868, May 2019.

[27] A. Kyriacou, P. Demetriou, C. Panayiotou, and E. Kyriakides, "Controlled islanding solution for large-scale power systems," *IEEE Trans. Power Syst.*, vol. 33, no. 2, pp. 1591–1602, Mar. 2018.

[28] C. Wang, B. Zhang, Z. Hao, J. Shu, P. Li, and Z. Bo, "A novel real-time searching method for power system splitting boundary," *IEEE Trans. Power Syst.*, vol. 25, no. 4, pp. 1902–1909, Nov. 2010.

[29] F. Znidi, H. Davarikia, K. Iqbal, and M. Barati, "Multi-layer spectral clustering approach to intentional islanding in bulk power systems," *J. Modern Power Syst. Clean Energy*, vol. 7, no. 5, pp. 1044–1055, 2019.

[30] M. R. Aghamohammadi and A. Shahmohammadi, "Intentional islanding using a new algorithm based on ant search mechanism," *Int. J. Elect. Power Energy Syst.*, vol. 35, no. 1, pp. 138–147, 2012.

[31] M. H. Oboudi, M. Mohammadi, and M. Rastegar, "Resilience-oriented intentional islanding of reconfigurable distribution power systems," *J. Modern Power Syst. Clean Energy*, vol. 7, no. 4, pp. 741–752, 2019.

[32] E. M. Gui and I. MacGill, "Typology of future clean energy communities: An exploratory structure, opportunities, and challenges," *Energy Res. Social Sci.*, vol. 35, pp. 94–107, 2018.

[33] B. Astarloa, A. Kaakeh, M. Lombardi, and J. Scalise, "Future of electricity: New technologies transforming the grid edge," World Econ. Forum, Cologny, Switzerland, Tech. Rep., 2017.

[34] "Directive 2018/2001 of the European parliament and of the council on the promotion of the use of energy from renewable sources," 2018.

[35] A. Shrestha et al., "Peer-to-Peer energy trading in micro/mini-grids for local energy communities: A review and case study of Nepal," *IEEE Access*, vol. 7, pp. 131911–131928, 2019.

[36] M. Coraggio, S. Jafarpour, F. Bullo, and M. d. Bernardo, "Minimax flow over acyclic networks: Distributed algorithms and microgrid application," *IEEE Trans. Control Netw. Syst.*, 2022, early access, doi: 10.1109/TCNS.2022.3212638.

[37] E. Espina, J. Llanos, C. Burgos-Mellado, R. Cárdenas-Dobson, M. Martínez-Gómez, and D. Sáez, "Distributed control strategies for microgrids: An overview," *IEEE Access*, vol. 8, pp. 193412–193448, 2020.

[38] P. Kundur et al., "Definition and classification of power system stability IEEE/CIGRE joint task force on stability terms and definitions," *IEEE Trans. Power Syst.*, vol. 19, no. 3, pp. 1387–1401, Aug. 2004.

[39] S. A. Arefifar, Y. A.-R. I. Mohamed, and T. H. M. El-Fouly, "Supply-adequacy-based optimal construction of microgrids in smart distribution systems," *IEEE Trans. Smart Grid*, vol. 3, no. 3, pp. 1491–1502, Sep. 2012.

[40] W. A. Kirk and B. Sims, "Handbook of metric fixed point theory," *Australian Mathematical Society Gazette*, vol. 29, no. 2. Berlin, Germany: Springer, 2002.

[41] U. of Washington College of Engineering, "Power systems test case archive," Accessed on: Jan., 17, 2021. [Online]. Available: http://labs.ece.uw.edu/pstca/

[42] R. D. Zimmerman, C. E. Murillo-Sánchez, and R. J. Thomas, "MATPOWER: Steady-state operations, planning, and analysis tools for power systems research and education," *IEEE Trans. Power Syst.*, vol. 26, no. 1, pp. 12–19, Feb. 2011.

[43] J. W. Bialek and V. Vahidinasab, "Tree-partitioning as an emergency measure to contain cascading line failures," *IEEE Trans. Power Syst.*, vol. 37, no. 1, pp. 467–475, Jan. 2022.

[44] T. H. Cormen, C. E. Leiserson, R. L. Rivest, and C. Stein, *Introduction to Algorithms*. Cambridge, MA, USA: MIT, 2009.
[45] J. Quirós-Tortós, P. Demetriou, M. Panteli, E. Kyriakides, and V. Terzija, "Intentional controlled islanding and risk assessment: A unified framework," *IEEE Syst. J.*, vol. 12, no. 4, pp. 3637–3648, Dec. 2018.
[46] P. Demetriou, M. Asprou, and E. Kyriakides, "A real-time controlled islanding and restoration scheme based on estimated states," *IEEE Trans. Power Syst.*, vol. 34, no. 1, pp. 606–615, Jan. 2019.

Francesco Lo Iudice (Member, IEEE) received the master's degree in management engineering, and the Ph.D. degree in automation and computer science from the University of Naples Federico II, Naples, Italy, in 2012 and 2016, respectively.

He is currently an Associate Professor of automatic control with the Department of Electrical Engineering and Information Technologies, University of Naples Federico II. During his Ph.D. and his year as a Postdoctoral Research Fellow, he spent a year with the Department of Mechanical Engineering, University of New Mexico, Albuquerque, NM, USA, where he was a Research Fellow in 2015. His current research interests include synchronization, controllability and control of complex networks, with applications to the fields of opinion dynamics in large social groups, control of power grids, and formation control.

Ricardo Cardona-Rivera received the bachelor's degree in electronic engineering and M.S. degree in automation engineering from the National University of Colombia, Bogota, Colombia, in 2015 and 2018, respectively, and the Ph.D. degree in information technology and electrical engineering from the University of Naples Federico II, Naples, Italy, in 2022.

He was previously associated with the National University of Columbia. He is currently a Postdoctoral Fellow with the Center of Translational Neurophysiology, Italian Institute of Technology, Genoa, Italy. His current research interests include the analysis and control of complex systems and its applications in power systems and neuroscience.

Antonio Grotta received the master's degree in automation engineering from the University of Naples Federico II, Naples, Italy, in 2020. He is currently working toward the Ph.D. degree in data driven control for multi-agent systems with the Scuola Superiore Meridionale, School for Advanced Studies, Naples, Italy.

In 2021, he was a Research Fellow with the University of Naples Federico II. His current research interests include complex networks and artificial intelligence.

Marco Coraggio (Member, IEEE) received the Ph.D. degree in information technology and electrical engineering from the University of Naples Federico II, Naples, Italy, in 2020.

He was a Visiting Student with the University of Bristol, Bristol, U.K., in 2016, and with the University of California, Santa Barbara, CA, USA, in 2019. From 2020 to 2021, he was a Postdoctoral Fellow with the University of Naples Federico II and has been a Postdoctoral Fellow with the Scuola Superiore Meridionale, School for Advanced Studies, Naples, since 2021. His current research interests include complex networks and applications, data-driven control, and piecewise-smooth and hybrid dynamical systems.

Mario di Bernardo (Fellow, IEEE) received the M.Sc. degree in automation engineering from the University of Naples Federico II, Naples, Italy in 1995 and the Ph.D. degree in applied nonlinear mathematics from the University of Bristol, Bristol, U.K., in 1998.

He is currently Professor of Automatic Control with the University of Naples Federico II, Naples, Italy, and a Visiting Professor of Nonlinear Systems and Control with the University of Bristol, Bristol, U.K. He currently serves as Deputy Provice Chancellor for internationalization of the University of Naples Federico II and coordinates the research area on Modeling and Engineering Risk and Complexity of the Scuola Superiore Meridionale, the New School for Advanced Studies, located in Naples, Italy. He authored or coauthored more than 220 international scientific publications including more than 110 papers in scientific journals, a research monograph, and two edited books. According to the international database SCOPUS (March 2023), his h-index is 53 and his publications received over 11 000 citations by other authors. His research interests include the analysis and control of collective behavior in complex systems, piecewise-smooth dynamical systems, nonlinear dynamics and nonlinear control with applications to engineering and life science.

Dr. di Bernardo was bestowed the title of Cavaliere of the Order of Merit of the Italian Republic for scientific merits from the President of Italy in 2007. He was elevated to the grade of Fellow of the IEEE in 2012 for his contributions to the analysis, control, and applications of nonlinear systems and complex networks. He served as President of the Italian Society for Chaos and Complexity, as a Member of the Board of Governors of the IEEE Circuits and Systems Society, Vice President for Financial Activities of the society, and as a Member of the Board of Governors of the IEEE Control Systems Society.